

Learning to Select Pre-Trained Deep Representations with Bayesian Evidence Framework

Yong-Deok Kim, Taewoong Jang, Bohyung Hang, Seungjin Choi

Department of Computer Science and Engineering
Pohang University of Science and Technology, Korea
{karma13, tw.jang, bhhan, seungjin}@postech.ac.kr

Abstract

We propose a Bayesian evidence framework to facilitate transfer learning from pre-trained deep convolutional neural networks (CNNs). Our framework is formulated on top of a least squares SVM (LS-SVM) classifier, which is simple and fast in both training and testing and achieves competitive performance in practice. The regularization parameters in LS-SVM is estimated automatically without grid search and cross-validation by maximizing evidence, which is a useful measure to select the best performing CNN out of multiple candidates for transfer learning; the evidence is optimized efficiently by employing Aitken's delta-squared process, which accelerates convergence of fixed point update. The proposed Bayesian evidence framework also provides a good solution to identify the best ensemble of heterogeneous CNNs through a greedy algorithm. Our Bayesian evidence framework for transfer learning is tested on 12 benchmark visual recognition datasets and illustrates the state-of-the-art performance consistently in terms of prediction accuracy and modeling efficiency.

1. Introduction

Deep convolutional neural network (CNN) has drawn great attention in machine learning and computer vision communities because a lot of outstanding results have been reported recently in visual recognition problems [17, 25], several deep CNN models trained on large scale image repositories such as ImageNet [8] are open to public, and high-performance computing systems such as GPUs and distributed clusters have become available

Moreover, image representations from deep CNN models trained for specific image classification tasks turn out to be powerful even for general purposes [2, 7, 9, 21, 23] and consequently useful for transfer learning or domain adaptation. As a result, fine-tuning of CNN trained on a specific problem or dataset has been performed to facilitate train-

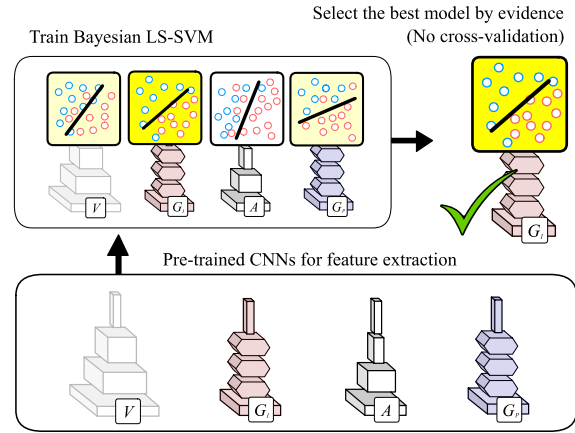


Figure 1. We address a problem to select the best CNN out of multiple candidates as shown in this figure. Additionally, our algorithm is capable of identifying the best ensemble of multiple CNNs to further improve performance.

ing for new tasks or domains [15, 7, 2, 38] and the application of off-the-shelf classification algorithms such as SVM to the representations from deep CNNs [9] is getting more attractive in many computer vision problems. However, fine-tuning of an entire deep network still requires a lot of efforts and resources, and SVM-based methods involve time consuming grid search and cross validation to identify good regularization parameters. In addition, when multiple pre-trained deep CNN models are available, it is ambiguous which pre-trained models are appropriate for representation in target tasks and which classifiers are ideal to maximize accuracy and efficiency. Unfortunately, most existing techniques for transfer learning or domain adaptation are limited to empirical analysis or ad-hoc application specific approaches.

We propose a simple but effective algorithm for transfer learning from pre-trained deep CNNs based on Bayesian least squares SVM (LS-SVM), which is formulated with

Bayesian evidence framework [18, 31] and LS-SVM [28]¹. This approach automatically determines regularization parameters in a principled way, and shows comparable performance to the standard SVMs based on hinge loss or squared hinge loss. More importantly, Bayesian LS-SVM provides an effective solution to select the best CNN out of multiple candidates and identify a good ensemble of heterogeneous CNNs for performance improvement. Our approach is illustrated in Figure 1.

We also propose a fast Bayesian LS-SVM, which maximizes the evidence more efficiently based on Aitken’s delta-squared process [1]. Considering simplicity and accuracy, we claim that our fast Bayesian LS-SVM is a reasonable choice for transfer learning with deep learning representation in visual recognition problems. Based on this approach, we achieved very promising results compared to the state-of-the-art techniques on 12 famous visual recognition tasks.

The rest of this paper is organized as follows. Section 2 describes examples of transfer learning or domain adaptation based on pre-trained CNNs for visual recognition problems. Then, we discuss Bayesian evidence framework applicable to the same problem in Section 3 and its acceleration technique using Aitken’s delta-squared process in Section 4. The performance of our algorithm in various applications is demonstrated in Section 5.

2. Related Work

Since *AlexNet* [17] demonstrated surprisingly impressive performance in the ImageNet large scale visual recognition challenge (LSVRC) 2012, a few deep CNNs with different architectures, *e.g.*, VGG [26] and GoogLeNet [29], have been proposed in the subsequent events. All of these three networks were trained independently although they used the same dataset.

Instead of training deep CNNs from scratch, some people have attempted to refine pre-trained networks for new tasks or datasets by updating the weights of all neurons or adopt the intermediate outputs of existing deep networks as generic visual feature descriptors. These strategies can be interpreted as transfer learning or domain adaptation.

Refining a pre-trained CNN is called fine-tuning, where the architecture of the network may be preserved while weights are updated based on new training data. Fine-tuning is generally useful to improve performance [15, 7, 2, 38] but requires careful implementation to avoid overfitting. The second approach regards the pre-trained CNNs as feature extraction machines and combines the deep representations with the off-the-shelf classifiers such as linear SVM [9, 36], logistic regression [9, 36], and multi-layer neural network [21]. The outputs from the first or second

fully connected layers are typically used as feature descriptors. The techniques in this category are successful in many visual recognition tasks [23, 2], where the third-last activations of *OverFeat* [25] are employed as generic image representations.

When combining a classification algorithm with image representations from pre-trained deep CNNs, we often face a critical issue. Although several deep CNN models trained on large scale image repositories such as ImageNet [8] and Places [40] are publicly available, there is no principled way to select a CNN out of multiple candidates and find the best ensemble of multiple CNNs for performance optimization. Note that existing algorithms typically rely on trial-and-error approaches for model selection and fail to provide clear evidence for superior performance [2].

We present an effective and efficient way to select a CNN and ensemble multiple pre-trained CNNs for new tasks or datasets. Our model selection algorithm is based on a combination of Bayesian evidence framework [18] and LS-SVM classifier [28], which formulates Bayesian LS-SVM [31]. This technique has capability to identify a good regularization parameter automatically. Cross validation is frequently adopted for the same purposes, but requires time consuming grid search and multi-fold evaluation. Random search [3] or Bayesian optimization [27] may be more effective for model selection in high-dimensional hyperparameter space than grid search, but we deal with 1D regularization parameter search in this paper, where our algorithm is still more reliable and efficient.

One may argue against the use of LS-SVM for classification because the least squares loss function in LS-SVM tends to penalize well-classified examples. However, least squares loss is often used for training multi-layer perceptron [5] and shows comparable performance to SVMs [30, 39]. More importantly, Bayesian LS-SVM provides a technically sound formulation with outstanding performance in terms of speed and accuracy for transfer learning with deep representations.

3. Bayesian LS-SVM for Model Selection

This section discusses a Bayesian evidence framework to select the best CNN model(s) in the presence of transferable multiple candidates and identify a reasonable regularization parameter for LS-SVM classifier automatically.

3.1. Problem Definition and Formulation

Suppose that we have a set of pre-trained deep CNN models denoted by $\{\text{CNN}_m, m = 1 \dots M\}$. Our goal is to identify the best performing deep CNN model among the M networks for transfer learning. A naïve approach is to perform fine tuning of network for target task, which requires substantial efforts for training. Another option is to replace some of fully connected layers in a CNN with an

¹This is also known as a regularized least squares classifier [24], is similar to SVM but involves a least square loss.

off-the-shelf classifier such as SVM and check performance of target task through regularization parameter search and cross-validation for each network, which would be computationally expensive.

We adopt a Bayesian evidence framework based on LS-SVM to achieve the goal in a principled way, where the evidence of each network is maximized iteratively and the maximum evidences are used to select a reasonable model. During the evidence maximization procedure, the regularization parameter of LS-SVM is identified automatically without time consuming grid search and cross-validation. In addition, the Bayesian evidence framework is also applied to the construction of an ensemble of multiple CNNs to accomplish further performance improvement.

3.2. LS-SVM

Before describing Bayesian evidence framework, we review the formulation of LS-SVM. We deal with multi-label or multi-class classification problem, where the number of categories is K . Let $\mathcal{D} = \{(\mathbf{x}_n, \mathbf{y}_n^{(k)}), k = 1 \dots K\}_{n=1 \dots N}$ be a training set, where $\mathbf{x}_n \in \mathbb{R}^D$ is a feature vector and $y_n^{(k)}$ is a binary variable that is set to 1 if label k is given to \mathbf{x}_n and 0 otherwise.

For each class k , we minimize a least squares loss with L_2 regularization penalty as follows:

$$\min_{\mathbf{w}^{(k)} \in \mathbb{R}^D} \|\mathbf{y}^{(k)} - \mathbf{X}^\top \mathbf{w}^{(k)}\|^2 + \lambda^{(k)} \|\mathbf{w}^{(k)}\|^2, \quad (1)$$

where $\mathbf{X} = [\mathbf{x}_1, \dots, \mathbf{x}_N] \in \mathbb{R}^{D \times N}$ and $\mathbf{y}^{(k)} = [y_1^{(k)}, \dots, y_N^{(k)}]^\top \in \mathbb{R}^N$. The optimal solution of the problem in (1) is given by

$$\mathbf{w}^{(k)} = (\mathbf{X}\mathbf{X}^\top + \lambda^{(k)}\mathbf{I})^{-1} \mathbf{X}\mathbf{y}^{(k)}, \quad (2)$$

where \mathbf{I} is an identity matrix. This regularized least squares approach has clear benefit that it requires only one eigen-decomposition of $\mathbf{X}\mathbf{X}^\top$ to obtain the solution in (2) for all combinations of $\lambda^{(k)}$ and $\mathbf{y}^{(k)}$.

3.3. Bayesian Evidence Framework

The optimization of the regularized least squares formulation presented in (1) is equivalent to the maximization of the posterior with fixed hyperparameters α and β denoted by $p(\mathbf{w}|\mathbf{y}, \mathbf{X}, \alpha, \beta)$, where $\lambda = \alpha/\beta$. The posterior can be decomposed into two terms by Bayesian theorem as

$$p(\mathbf{w}|\mathbf{y}, \mathbf{X}, \alpha, \beta) \propto p(\mathbf{y}|\mathbf{X}, \mathbf{w}, \beta)p(\mathbf{w}|\alpha), \quad (3)$$

where $p(\mathbf{y}|\mathbf{X}, \mathbf{w}, \beta)$ corresponds to Gaussian observation noise model given by

$$p(\mathbf{y}|\mathbf{X}, \mathbf{w}, \beta) = \prod_{n=1}^N \mathcal{N}(\mathbf{y}_n | \mathbf{x}_n^\top \mathbf{w}, \beta^{-1} \mathbf{I}) \quad (4)$$

and $p(\mathbf{w}|\alpha)$ denotes a zero-mean isotropic Gaussian prior given by

$$p(\mathbf{w}|\alpha) = \mathcal{N}(\mathbf{w} | \mathbf{0}, \alpha^{-1} \mathbf{I}). \quad (5)$$

Note that we dropped superscript (k) for notational simplicity from the equations in this subsection.

In the Bayesian evidence framework [18, 31], the evidence, also known as marginal likelihood, is a function of hyperparameters α and β as

$$p(\mathbf{y}|\mathbf{X}, \alpha, \beta) = \int p(\mathbf{y}|\mathbf{X}, \mathbf{w}, \beta)p(\mathbf{w}|\alpha)d\mathbf{w}. \quad (6)$$

Under the probabilistic model assumptions corresponding to (4) and (5), the log evidence $\mathcal{L}(\alpha, \beta)$ is given by

$$\begin{aligned} \mathcal{L}(\alpha, \beta) &\equiv \log p(\mathbf{y}|\mathbf{X}, \alpha, \beta) \\ &= \frac{D}{2} \log \alpha + \frac{N}{2} \log \beta - \frac{1}{2} \log |\mathbf{A}| \\ &\quad - \frac{\beta}{2} \|\mathbf{y} - \mathbf{X}^\top \mathbf{m}\|^2 - \frac{\alpha}{2} \mathbf{m}^\top \mathbf{m} - \frac{N}{2} \log 2\pi, \end{aligned} \quad (7)$$

where the precision matrix and mean vector of the posterior $p(\mathbf{w}|\mathbf{y}, \mathbf{X}, \alpha, \beta) = \mathcal{N}(\mathbf{w}|\mathbf{m}, \mathbf{A}^{-1})$ are given respectively by

$$\mathbf{A} = \alpha \mathbf{I} + \beta \mathbf{X}\mathbf{X}^\top \text{ and } \mathbf{m} = \beta \mathbf{A}^{-1} \mathbf{X}\mathbf{y}.$$

The log evidence $\mathcal{L}(\alpha, \beta)$ is maximized by repeatedly alternating the following fixed point update rules

$$\alpha = \frac{\gamma}{\mathbf{m}^\top \mathbf{m}} \text{ and} \quad (8)$$

$$\beta = \frac{N - \gamma}{\|\mathbf{y} - \mathbf{X}^\top \mathbf{m}\|^2}, \quad (9)$$

which involves the derivation of γ as

$$\gamma = \sum_{d=1}^D \frac{\beta s_d}{\alpha + \beta s_d} = \sum_{d=1}^D \frac{s_d}{\lambda + s_d}, \quad (10)$$

where $\{s_d\}_{d=1}^D$ are eigenvalues of $\mathbf{X}\mathbf{X}^\top$. Note that \mathbf{m} and γ should be re-estimated after each update of α and β .

Another pair of update rules of α and β are derived by an expectation-maximization (EM) technique as

$$\alpha = \frac{D}{\mathbf{m}^\top \mathbf{m} + \text{Tr}(\mathbf{A}^{-1})} \text{ and} \quad (11)$$

$$\beta = \frac{N}{\|\mathbf{y} - \mathbf{X}^\top \mathbf{m}\|^2 + \text{Tr}(\mathbf{A}^{-1} \mathbf{X}\mathbf{X}^\top)}, \quad (12)$$

but these procedures are substantially slower than the fixed point update rules in (8) and (9).

Through the optimization procedures described above, we determine the regularization parameter $\lambda = \alpha/\beta$. Although the estimated parameters are not optimal, they may still be reasonable solutions since they are obtained by maximizing marginal likelihood in (6).

3.4. Model Selection using Evidence

The evidence computed in the previous subsection is for a single class, and the overall evidence for entire classes, denoted by \mathcal{L}^* , is obtained by the summation of the evidences from individual classes, which is given by

$$\mathcal{L}^* = \sum_{k=1}^K \mathcal{L}(\alpha^{(k)}, \beta^{(k)}). \quad (13)$$

We compute the overall evidence corresponding to each deep CNN model, and choose the model with the maximum evidence for transfer learning. We expect that the selected model perform best among all candidate models, which will be verified in our experiment. In addition, when an ensemble of deep CNNs needs to be constructed for a target task, our approach selects a subset of good pre-trained CNNs in a greedy manner. Specifically, we add a network with the largest evidence in each stage and test whether the augmented network improves the evidence or not. The network is accepted if the evidence increases, or rejected otherwise. After the last candidate is tested, we obtain the final network combination and its associated model learned with the concatenated feature descriptors from accepted networks.

4. Fast Bayesian LS-SVM

Bayesian evidence framework discussed in Section 3 is useful to identify a good CNN for transfer learning and a reasonable regularization parameter. To make this framework even more practical, we present a faster algorithm to accomplish the same goal and a new theory that guarantees the converges of the algorithm.

4.1. Reformulation of Evidence

We are going to reduce $\mathcal{L}(\alpha, \beta)$ to a function with only one parameter that directly corresponds to the regularization parameter $\lambda = \alpha/\beta$. To this end, we re-write $\mathcal{L}(\alpha, \beta)$ by using the eigen-decomposition $\mathbf{X}\mathbf{X}^\top = \mathbf{U}\mathbf{S}\mathbf{U}^\top$ as

$$\begin{aligned} \mathcal{L}(\alpha, \beta) = & \frac{D}{2} \log \alpha + \frac{N}{2} \log \beta - \frac{1}{2} \sum_{d=1}^D \log(\alpha + \beta s_d) \\ & - \frac{\beta}{2} \mathbf{y}^\top \mathbf{y} + \frac{\beta^2}{2} \sum_{d=1}^D \frac{h_d^2}{\alpha + \beta s_d} - \frac{N}{2} \log 2\pi, \end{aligned} \quad (14)$$

where s_d is the d -th diagonal element in \mathbf{S} and h_d denotes the d -th element in $\mathbf{h} = \mathbf{U}^\top \mathbf{X}\mathbf{y}$. Then, we re-parameterize $\mathcal{L}(\alpha, \beta)$ into $\mathcal{F}(\lambda, \beta)$ as

$$\begin{aligned} \mathcal{F}(\lambda, \beta) = & \frac{D}{2} \log \lambda + \frac{N}{2} \log \beta - \frac{1}{2} \sum_{d=1}^D \log(\lambda + s_d) \\ & - \frac{\beta}{2} \left(\mathbf{y}^\top \mathbf{y} - \sum_{d=1}^D \frac{h_d^2}{\lambda + s_d} \right) - \frac{N}{2} \log 2\pi. \end{aligned} \quad (15)$$

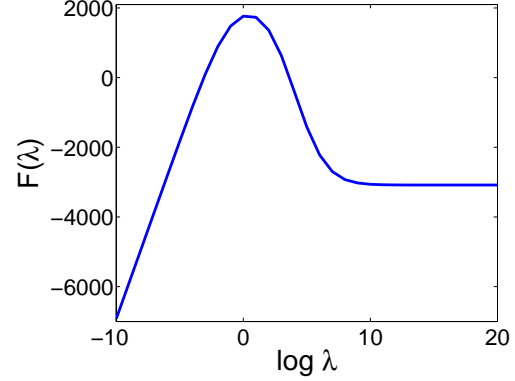


Figure 2. Plot of the log evidence $\mathcal{F}(\lambda)$ with respect to $\log \lambda$.

The derivative of $\mathcal{F}(\lambda, \beta)$ with respect to β is given by

$$\frac{\partial \mathcal{F}}{\partial \beta} = \frac{N}{2\beta} - \frac{1}{2} \left(\mathbf{y}^\top \mathbf{y} - \sum_{d=1}^D \frac{h_d^2}{\lambda + s_d} \right),$$

and we obtain the following equation by setting this derivative to zero,

$$\beta = \frac{N}{\mathbf{y}^\top \mathbf{y} - \sum_{d=1}^D \frac{h_d^2}{\lambda + s_d}}. \quad (16)$$

Finally, we obtain a one-dimensional function of the log evidence by plugging (16) into (15), which is given by

$$\begin{aligned} \mathcal{F}(\lambda) = & \frac{1}{2} \sum_{d=1}^D \log \frac{\lambda}{\lambda + s_d} + \frac{N}{2} \log N - \frac{N}{2} - \frac{N}{2} \log 2\pi \\ & - \frac{N}{2} \log \left(\mathbf{y}^\top \mathbf{y} - \sum_{d=1}^D \frac{h_d^2}{\lambda + s_d} \right). \end{aligned} \quad (17)$$

Figure 2 illustrates the curvature of this log evidence function with respect to $\log \lambda$.

4.2. New Fixed-point Update Rule

We now derive a new fixed point update rule maximizing (17) and present the sufficient condition for the existence of a fixed point.

The stationary points in (17) with respect to λ satisfy

$$\frac{1}{2} \sum_{d=1}^D \frac{s_d}{\lambda(\lambda + s_d)} - \frac{N}{2} \frac{\sum_{d=1}^D \frac{h_d^2}{(\lambda + s_d)^2}}{\mathbf{y}^\top \mathbf{y} - \sum_{d=1}^D \frac{h_d^2}{\lambda + s_d}} = 0, \quad (18)$$

and the fixed-point update equation is obtained by maximizing (17) as

$$\lambda = \frac{\sum_{d=1}^D \frac{s_d}{\lambda + s_d}}{\left(\mathbf{y}^\top \mathbf{y} - \sum_{d=1}^D \frac{h_d^2}{\lambda + s_d} \right) \left(\sum_{d=1}^D \frac{h_d^2}{(\lambda + s_d)^2} \right)}. \quad (19)$$

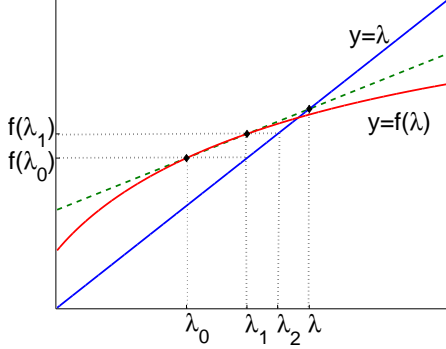


Figure 3. Illustration of Aitken's delta-squared process. The fixed point update function $f(\lambda)$ is approximated by green dashed line and its intersection with $y = \lambda$ becomes the next update point.

As illustrated in Figure 2, $\mathcal{F}(\lambda)$ in (17) is neither a convex nor concave function. However, we can show the sufficient condition of the existence of the fixed point using the following theorem.

Theorem 1. Denote the update rule in (19) by $f(\lambda)$. If \mathbf{y} is a binary variable and \mathbf{x}_n is an L_2 normalized nonnegative vector, then $f(\lambda)$ has a fixed point.

Proof. We first show that $f(\lambda)$ is a asymptotically linear as

$$\begin{aligned} \lim_{\lambda \rightarrow \infty} \frac{f(\lambda)}{\lambda} &= \lim_{\lambda \rightarrow \infty} \frac{\left(\mathbf{y}^\top \mathbf{y} - \sum_{d=1}^D \frac{h_d^2}{\lambda + s_d} \right) \sum_{d=1}^D \frac{s_d}{\lambda + s_d}}{\lambda N \sum_{d=1}^D \frac{h_d^2}{(\lambda + s_d)^2}} \\ &= \frac{\mathbf{y}^\top \mathbf{y} \sum_{d=1}^D s_d}{N \sum_{d=1}^D h_d^2} = \frac{\|\mathbf{y}\|^2 \|\mathbf{X}\|_F^2}{N \|\mathbf{X}\mathbf{y}\|^2}. \end{aligned}$$

Since \mathbf{y} is binary and \mathbf{x}_n is L_2 normalized and nonnegative, we can derive the following two relations,

$$\|\mathbf{y}\|^2 \|\mathbf{X}\|_F^2 = PN \quad \text{and} \quad (20)$$

$$\|\mathbf{X}\mathbf{y}\|^2 = \left(\sum_{n:y_n=1} x_n \right)^2 > \sum_{n:y_n=1} x_n^2 = P, \quad (21)$$

where $P = \sum_{n=1}^N y_n$. From (20) and (21), it is shown that $\|\mathbf{y}\|^2 \|\mathbf{X}\|_F^2 < N \|\mathbf{X}\mathbf{y}\|^2$.

Obviously, $f(0) > 0$ and there exists a λ^+ such that $f(\lambda^+) < \lambda^+$. The intermediate value theorem implies the existence of λ^* such that $f(\lambda^*) = \lambda^*$, where $0 < \lambda^* < \lambda^+$ as illustrated in Figure 3. \square

The fixed point is unique if $f(\lambda)$ is concave; according to our observation, $f(\lambda)$ is always concave. However, unfortunately, we have no proof of it yet and we remain this problem as the future work.

Algorithm 1 Fast Bayesian Least Squares

Input: $\mathbf{X} \in \mathbb{R}^{N \times D}$ and $\mathbf{y} \in \mathbb{R}^N$.
Output: Optimal solutions (\mathbf{w}, λ) .
Initialize λ // e.g., $\lambda = 1$
 $(\mathbf{U}, \mathbf{S}) \leftarrow \text{eigen-decomposition}(\mathbf{X}\mathbf{X}^\top)$
 $\mathbf{s} \leftarrow \text{diag}(\mathbf{S})$
 $\mathbf{h} \leftarrow \mathbf{U}^\top \mathbf{X}\mathbf{y}$
repeat
 $\lambda_0 \leftarrow \lambda$
 $\lambda_1 \leftarrow \text{UPDATE}(\lambda_0, \mathbf{s}, \mathbf{h}, N, \mathbf{y}^\top \mathbf{y})$
 $\lambda_2 \leftarrow \text{UPDATE}(\lambda_1, \mathbf{s}, \mathbf{h}, N, \mathbf{y}^\top \mathbf{y})$
 $\lambda \leftarrow \lambda_0 - \frac{(\lambda_1 - \lambda_0)^2}{(\lambda_2 - \lambda_1) - (\lambda_1 - \lambda_0)}$
if $\lambda < 0$ or $\lambda = \pm\infty$ **then**
 $\lambda \leftarrow \lambda_2$
end if
until $|\lambda - \lambda_0| < \epsilon$ // e.g., $\epsilon = 10^{-5}$
 $\mathbf{w} \leftarrow \mathbf{U}(\mathbf{S} + \lambda \mathbf{I})^{-1} \mathbf{h}$

Algorithm 2 $\lambda = \text{UPDATE}(\lambda, \mathbf{s}, \mathbf{h}, N, \mathbf{y}^\top \mathbf{y})$

$\gamma \leftarrow \sum_{d=1}^D \frac{s_d}{\lambda + s_d}$
 $\beta \leftarrow N / (\mathbf{y}^\top \mathbf{y} - \sum_{d=1}^D \frac{h_d^2}{\lambda + s_d})$
 $\mathbf{m}^\top \mathbf{m} \leftarrow \sum_{d=1}^D \frac{h_d^2}{(\lambda + s_d)^2}$
 $\lambda \leftarrow \frac{\gamma}{\beta \mathbf{m}^\top \mathbf{m}}$
return λ

4.3. Speed Up Algorithm

We accelerate the fixed point update rule in (19) by using Aitken's delta-squared process [1]. Figure 3 illustrates the Aitken's delta-squared process. Let's focus on the two points $(\lambda_0, f(\lambda_0))$ and $(\lambda_1, f(\lambda_1))$, and line going through these two points. The equation of this line is

$$y = \lambda_1 + (\lambda - \lambda_0) \frac{\lambda_2 - \lambda_1}{\lambda_1 - \lambda_0}, \quad (22)$$

where $f(\lambda_0)$ and $f(\lambda_1)$ are replaced by λ_1 and λ_2 , respectively. The idea behind Aitken's method is to approximate fixed point λ^* using the intersection of the line in (22) with line $y = \lambda$, which is given by

$$\lambda = \lambda_0 - \frac{(\lambda_1 - \lambda_0)^2}{(\lambda_2 - \lambda_1) - (\lambda_1 - \lambda_0)}. \quad (23)$$

Our fast Bayesian learning algorithm for the regularized least squares problem in (1) is summarized in Algorithm 1. In our algorithm, we first compute the eigen-decomposition of $\mathbf{X}\mathbf{X}^\top$. This is the most time consuming part but needs to be performed only once since the result can be reused for every label in \mathbf{y} . After that, we obtain the regularization parameter λ through an iterative procedure.

When we apply the Aitken's delta-squared process, we have two potential failure cases as illustrated in Figure 4(a)

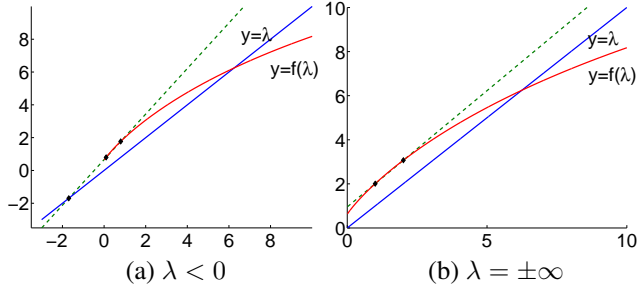


Figure 4. Two failure cases of Aitken’s delta-squared process. (a) The first case arises if initial λ_0 is far from the fixed point λ^* , which results in $\lambda < 0$. (b) The second case occurs when approximating line (dashed green) is parallel to $y = \lambda$, where $\lambda = \pm\infty$.

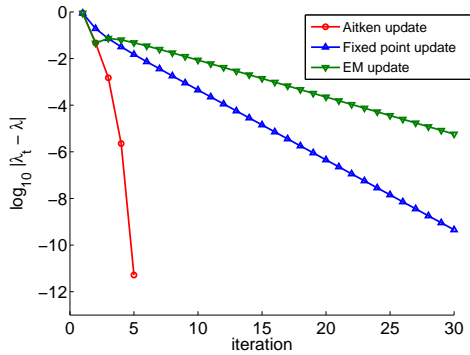


Figure 5. Comparison between Aitken’s delta-squared process, fixed point update rules, and EM update rules on PASCAL VOC 2012 dataset (class = *aeroplane*). Aitken’s delta-squared process significantly faster than other methods.

and 4(b). The first case often arises if the initial λ_0 is far from the fixed point λ^* , and the second case occurs when the approximating line in (22) is parallel to $y = \lambda$. Fortunately, these failures rarely happen in practice and can be handled easily by skipping the procedure in (23) and updating λ with λ_2 .

Figure 5 demonstrates the relative convergence rates of three different techniques—Aitken’s delta-squared process in Algorithm 1, fixed point update rules in (8) and (9), and EM update method in (11) and (12). As illustrated in the figure, the Aitken’s delta-squared process requires a few iterations and is significantly faster than others.

5. Experiments

We present the details of our experiment setting and the performance of our algorithm compared to the state-of-the-art techniques in 12 visual recognition benchmark datasets.

5.1. Datasets and Image Representation

The 12 benchmark datasets include various visual recognition tasks such as object recognition, photo annotation, scene recognition, fine grained recognition, visual attribute

detection, and action recognition. Table 1 presents the characteristics of the datasets. We follow the given train and test split and evaluation measure of each dataset. For the datasets with bounding box annotations such as CUB200-2011, UIUC object attribute, Human attribute, and Stanford 40 actions, we enlarged the bounding boxes by 150% to consider neighborhood context as discussed in [23, 2].

For deep learning representation, we selected four pre-trained CNNs in the Berkeley’s Caffe Model Zoo: Princeton’s *GoogLeNet* [33], Oxford’s *VGG19* [26], and Berkeley’s *AlexNet* [9] trained on ImageNet, and Princeton’s *GoogLeNet* trained on Places [33]. We used the activations of the first fully connected layer, and the feature dimensions are 1024 in *GoogLeNet* and 4096 in *VGG19* and *AlexNet*.

Our implementation is in Matlab2011a, and all experiments were conducted on a quad-core Intel(R) core(TM) i7-3820 @ 3.60GHz processor.

5.2. Bayesian LS-SVM vs. SVM

We first compare the performance of our Bayesian LS-SVM with the standard SVM when they are applied to deep CNN features for visual recognition problems. We used only a single image scale 256×256 in this experiment. LIBLINEAR [12] package is used for SVM training and the regularization parameters are selected by grid search with cross validations.

Table 2 presents the complete results of our experiment. Bayesian LS-SVM is competitive to SVM in terms of prediction accuracy even with significantly reduced training time. Training SVM is getting slower than Bayesian LS-SVM as the number of classes increases so it is particularly slow in Caltech 256 and SUN 397 datasets.

Another notable observation in Table 2 is that the order of prediction accuracy is highly correlated to the evidence. This means that the selected model by Bayesian LS-SVM produces reliable testing accuracy and a proper deep learning image representation is obtained without time consuming grid search and cross validation. Note that cross validations in LS-SVM and SVM play the same role, but are less reliable and slower than our Bayesian evidence framework. The capability to select the appropriate CNN model and the corresponding regularization parameter is one of the most important properties of our algorithm.

5.3. Comparison with Other Methods

We now show that our Bayesian LS-SVM identifies a good combination of multiple CNNs and improves accuracy without grid search and cross validation.

For each task, we select a subset of the four pre-trained CNNs in a greedy manner as described in Section 3.4. Our algorithm is compared with DeCAF [9], Zeiler [36], INRIA [21], KTH-S [23], KTH-FT [2], VGG [26], Zhang [37, 38], and TUBFI [4]. In addition, our ensembles identified

Table 1. Characteristics of the 12 datasets. N_1 : number of training data, N_2 : number of test data, K : number of classes, L : average number of labels per image, AP: average precision, Acc.: accuracy, AUC: area under the ROC curve.

Dataset	Task	N_1	N_2	K	L	Box	Measure
PASCAL VOC 2007 [10]	object recognition	5011	4952	20	1.5		mean AP
PASCAL VOC 2012 [11]	object recognition	5717	5823	20	1.5		mean AP
Caltech 101 [14]	object recognition	3060	6086	102	1		mean Acc.
Caltech 256 [16]	object recognition	15420	15187	257	1		mean Acc.
ImageCLEF 2011 [20]	photo annotation	8000	10000	99	11.9		mean AP
MIT Indoor Scene [22]	scene recognition	5360	1340	67	1		mean Acc.
SUN 397 Scene [34]	scene recognition	19850	19850	397	1		mean Acc.
CUB 200-2011 [32]	fine-grained recognition	5994	5794	200	1	✓	mean Acc.
Oxford Flowers [19]	fine-grained recognition	2040	6149	200	1		mean Acc.
UIUC object attributes [13]	attribute detection	6340	8999	64	7.1	✓	mean AUC
Human attributes [6]	attribute detection	4013	4022	9	1.8	✓	mean AP
Stanford 40 actions [35]	action recognition	4000	5532	40	1	✓	mean AP

Table 3. Comparison to existing methods in all 12 datasets. The best ensembles identified by maximizing evidence through exhaustive search mostly coincide with the oracle combinations—the ones with the highest accuracy in test set, which is also identified by exhaustive search. The ensembles identified by our greedy search are very similar to the two exhaustive search methods and our algorithm consequently performs best in many tested datasets. (G₁: *GoogLeNet-ImageNet*, G_p: *GoogLeNet-Place*, V: *VGG19*, and A: *AlexNet*)

Method	VOC07	VOC12	CAL101	CAL256	CLEF	MIT	SUN	Birds	Flowers	UIUC	Human	Action
DeCAF	-	-	86.9	-	-	-	38.0	65.0	-	-	-	-
Zeiler	-	79.0	86.5	74.2	-	-	-	-	-	-	-	-
INRIA	77.7	82.8	-	-	-	-	-	-	-	-	-	-
KTH-S	71.8	-	-	-	-	64.9	49.6	62.8	90.5	90.6	73.8	58.9
KTH-FT	80.7	-	-	-	-	71.3	56.0	67.1	91.3	91.5	74.6	66.4
VGG	89.7	89.3	92.7	86.2	-	-	-	-	-	-	-	-
Zhang	-	-	-	-	-	-	-	76.4	-	-	79.0	-
TUBFI	-	-	-	-	44.3	-	-	-	-	-	-	-
Oracle (exhaustive)	G ₁ G _p V 90.0	G ₁ G _p V 89.4	G ₁ VA 95.3	G ₁ G _p VA 86.1	G ₁ G _p VA 55.7	G _p VA 84.9	G ₁ G _p VA 67.5	G ₁ VA 77.3	G ₁ G _p VA 94.7	G ₁ VA 92.0	G ₁ VA 80.8	G ₁ G _p V 78.6
Max evid. (exhaustive)	G ₁ G _p V 90.0	G ₁ G _p V 89.4	G ₁ VA 95.3	G ₁ G _p VA 86.1	G ₁ G _p V 55.5	G _p V 84.7	G _p V 67.5	G ₁ VA 77.3	G ₁ VA 94.5	G ₁ G _p VA 92.0	G ₁ VA 80.8	G ₁ G _p V 78.6
Ours (greedy)	G ₁ G _p V 90.0	G ₁ G _p V 89.4	G ₁ VA 95.3	G ₁ G _p VA 86.1	G ₁ G _p V 55.5	G _p V 84.7	G _p V 67.5	G ₁ VA 77.3	G ₁ VA 94.5	G ₁ G _p VA 92.0	G ₁ VA 80.8	G ₁ VA 77.8

by greedy evidence maximization are compared with the oracle combinations—the ones with the highest accuracy in test set found by exhaustive search—and the best combinations found by exhaustive evidence maximization.

Table 3 summarizes the results. We achieve the state-of-the-art performance in most of 12 tested problems through the ensembles based on the proposed algorithm. Our greedy ensembles are consistent with the selections by exhaustive evidence maximization and even oracle selections² made by testing accuracy maximization. Note that our network selection is natural and reasonable; *GoogLeNet-ImageNet* and *VGG19* are selected frequently except MIT and SUN, where *GoogLeNet-Place* is preferred to *GoogLeNet-ImageNet* since the two datasets are constructed for scene recognition.

²This option is practically impossible since it requires evaluation with test dataset using all available models for model selection.

6. Conclusion

We described a simple and efficient technique to transfer deep CNN models pre-trained on specific image classification tasks to another tasks. Our approach is based on Bayesian LS-SVM, which combines Bayesian evidence framework and SVM with a least squares loss. In addition, we presented a faster fixed point update rule for evidence maximization through Aitken’s delta-squared process. Our fast Bayesian LS-SVM obtained competitive results compared to the standard SVMs in the 12 benchmark datasets by selecting a good deep CNN model efficiently and estimating corresponding regularization parameters without grid search and cross validation. Moreover, we achieved the state-of-the-art performance by effectively identifying a reasonable ensemble of the candidate models through our Bayesian LS-SVM framework.

Table 2. Bayesian LS-SVM versus SVM. Without time consuming cross validation procedure, Bayesian LS-SVM achieves prediction accuracy competitive to SVM. In addition, Bayesian LS-SVM selects the proper CNN for each task by using the evidence. Best accuracy in LS-SVM and SVM denotes the maximum accuracy in test dataset using all learned models. Note that the selected model by Bayesian evidence framework or cross validation may not be the best one in testing. The following sets of regularization parameters are tested for cross validation in LS-SVM and SVM, respectively: $\{2^{-10}, 2^{-9}, \dots, 1, \dots, 2^9, 2^{10}\}$ and $\{0.01, 0.05, 0.1, 0.5, 1, 2, 5, 10\}$. (G₁: *GoogLeNet-ImageNet*, G_p: *GoogLeNet-Place*, V: *VGG19*, and A: *AlexNet*)

Dataset	CNN	LS-SVM						SVM		
		Best Accuracy	Bayesian			CV (5-fold, 21-grid)		Best Accuracy	CV (5-fold, 8-grid)	
		Accuracy	Evidence	Time	Accuracy	Time		Accuracy	Time	
VOC07	G ₁	85.3	85.2	46.9×10^3	1.1	85.2	8.4	85.0	84.7	122.4
	G _p	74.1	73.8	38.6×10^3	1.0	74.0	8.1	74.1	73.9	144.3
	V	85.9	85.8	48.0×10^3	41.9	85.8	172.2	85.9	85.8	257.5
	A	75.2	75.0	32.5×10^3	41.7	75.0	160.4	75.3	75.2	211.1
VOC12	G ₁	84.4	84.3	51.3×10^3	1.2	84.3	8.6	83.9	83.7	140.8
	G _p	73.2	72.9	40.6×10^3	1.1	73.1	8.4	73.2	73.1	170.7
	V	85.2	85.1	52.9×10^3	42.7	85.2	161.5	85.6	85.4	295.9
	A	74.1	73.9	34.3×10^3	42.7	74.0	161.8	74.4	74.3	160.7
CAL101	G ₁	90.6	90.0	37.8×10^4	1.0	89.6	6.0	91.4	85.1	325.0
	G _p	57.0	54.3	30.6×10^4	0.9	55.1	5.9	57.2	41.8	390.3
	V	92.2	92.1	40.9×10^4	31.5	88.8	142.7	92.2	86.8	729.4
	A	89.3	89.2	37.3×10^4	32.0	83.4	146.9	90.0	83.5	595.3
CAL256	G ₁	77.8	77.2	59.9×10^5	2.3	77.8	21.8	81.2	81.2	4060.4
	G _p	44.9	42.6	55.9×10^5	2.2	44.9	21.2	48.6	48.6	4991.8
	V	82.0	81.1	62.3×10^5	52.5	81.7	339.7	82.7	82.7	9653.1
	A	69.7	68.9	58.6×10^5	52.9	69.7	336.9	72.3	72.3	5348.6
CLEF	G ₁	49.1	48.9	20.5×10^4	1.5	48.8	37.0	47.7	47.4	1218.6
	G _p	47.5	47.1	20.8×10^4	1.4	47.1	36.9	47.1	46.7	1410.5
	V	50.7	50.3	21.3×10^4	45.9	50.4	248.5	50.4	50.1	2531.2
	A	44.8	44.6	18.7×10^4	46.1	44.6	245.9	44.4	44.1	2140.0
MIT	G ₁	66.7	66.0	30.1×10^4	1.2	66.7	5.8	69.4	69.2	400.9
	G _p	80.0	79.9	35.2×10^4	1.1	80.0	5.8	81.1	80.4	402.5
	V	73.2	73.1	31.1×10^4	42.6	73.2	186.8	74.7	74.7	895.5
	A	62.0	61.1	28.6×10^4	42.2	60.5	187.4	63.1	63.1	460.9
SUN	G ₁	48.1	47.0	12.8×10^6	3.1	48.1	36.5	54.2	54.2	8739.6
	G _p	61.1	60.1	13.2×10^6	2.9	61.1	34.4	63.3	63.3	8589.4
	V	55.0	53.7	12.9×10^6	57.4	54.9	419.8	57.1	57.1	20254.0
	A	45.4	44.9	12.7×10^6	50.8	45.4	419.0	48.6	48.6	10781.8
Birds	G ₁	65.2	64.3	15.6×10^5	1.3	64.1	11.0	67.6	56.5	1201.9
	G _p	16.4	13.6	14.9×10^5	1.5	15.0	11.1	16.8	11.1	1664.6
	V	69.2	68.6	15.8×10^5	44.1	61.5	259.2	71.1	59.4	2776.2
	A	59.0	58.5	15.5×10^5	45.3	46.6	257.9	61.4	51.6	1645.5
Flowers	G ₁	85.5	84.7	21.8×10^4	0.9	82.0	5.5	87.4	72.0	198.8
	G _p	55.6	51.7	19.4×10^4	0.9	51.8	5.5	57.1	32.8	234.7
	V	87.5	87.1	22.5×10^4	26.9	82.1	142.2	87.6	73.4	520.9
	A	87.6	87.6	22.9×10^4	27.3	81.8	146.7	88.3	77.1	271.3
UIUC	G ₁	91.5	90.3	13.5×10^4	1.4	90.9	8.0	91.3	90.6	605.5
	G _p	87.8	86.6	10.5×10^4	1.3	87.1	7.4	88.0	87.6	726.0
	V	92.5	91.1	14.4×10^4	43.8	92.0	186.3	92.2	91.7	1285.4
	A	91.4	89.9	12.9×10^4	44.1	91.0	191.2	90.8	90.5	683.7
Human	G ₁	76.0	75.8	-74.8×10^2	1.0	75.8	5.0	74.2	74.1	70.6
	G _p	58.7	58.4	-103.1×10^2	1.0	58.0	4.8	56.9	56.5	85.5
	V	75.4	75.1	-76.0×10^2	40.3	75.2	124.2	73.1	72.8	131.9
	A	71.9	71.3	-84.4×10^2	40.7	71.7	121.2	70.0	69.9	63.3
Action	G ₁	70.2	69.8	100.4×10^3	1.0	69.6	11.6	69.8	69.6	211.7
	G _p	48.3	47.6	86.5×10^3	1.1	47.9	11.4	48.2	47.7	246.2
	V	75.4	75.2	109.3×10^3	41.1	75.1	142.9	75.8	75.3	418.7
	A	58.0	57.7	89.6×10^3	41.5	57.5	156.5	57.4	57.1	206.8

References

- [1] A. C. Aitken. On Bernoulli's numerical solution of algebraic equations. *Proceedings of the Royal Society of Edinburgh*, 46:289–305, 1927. 2, 5
- [2] H. Azizpour, A. S. Razavian, J. Sullivan, A. Maki, and S. Carlsson. From generic to specific deep representations for visual recognition. *arXiv:1406.5774v2*, 2014. 1, 2, 6
- [3] J. Bergstra and Y. Bengio. Random search for hyper-parameter optimization. *Journal of Machine Learning Research*, 13(1):281–305, 2012. 2
- [4] A. Binder, W. Samek, M. Kloft, C. Müller, K.-R. Müller, and M. Kawanabe. The joint submission of the TU Berlin and Fraunhofer FIRST (TUBFI) to the ImageCLEF2011 photo annotation task. In *CLEF2011 Working Notes*, 2011. 6
- [5] C. M. Bishop. *Neural Networks for Pattern Recognition*. Clarendon press Oxford, 1995. 2
- [6] L. D. Bourdev, S. Maji, and J. Malik. Describing people: A poselet-based approach to attribute classification. In *ICCV*, 2011. 7
- [7] K. Chatfield, K. Simonyan, A. Vedaldi, and a. Zisserman. Return of the devil in the details: Delving deep into convolutional nets. In *BMVC*, 2014. 1, 2
- [8] J. Deng, W. Dong, R. Socher, L.-J. Li, K. Ki, and L. Fei-Fei. ImageNet: A large-scale hierarchical image database. In *CVPR*, 2010. 1, 2
- [9] J. Donahue, Y. Jia, O. Vinyals, J. Hoffman, n. Zhang, E. Tzeng, and T. Darrell. DeCAF: A deep convolutional activation feature for generic visual recognition. In *ICML*, 2014. 1, 2, 6
- [10] M. Everingham, L. V. Gool, C. K. I. Williams, J. Winn, and A. Zisserman. The PASCAL Visual Object Classes Challenge 2007 (VOC 2007) Results, 2007. 7
- [11] M. Everingham, L. V. Gool, C. K. I. Williams, J. Winn, and A. Zisserman. The PASCAL Visual Object Classes Challenge 2012 (VOC 2012) Results, 2012. 7
- [12] R. E. Fan, K. W. Chang, C. J. Hsieh, X. R. Wang, and C. J. Lin. LIBLINEAR: A library for large linear classification. *JMLR*, 9:1871–1874, 2008. 6
- [13] A. Farhadi, I. Endres, D. Hoiem, and D. A. Forsyth. Describing objects by their attributes. In *CVPR*, 2009. 7
- [14] L. Fei-Fei, R. Fergus, and P. Perona. Learning generative visual models from few training examples: An incremental bayesian approach tested on 101 object categories. *CVIU*, 106(1):59–70, 2007. 7
- [15] R. Girshick, J. Donahue, T. Darrell, and J. Malik. Rich feature hierarchies for accurate object detection and semantic segmentation. In *Proceedings of the IEEE International Conference on Computer Vision and Pattern Recognition (CVPR)*, pages 580–587. IEEE, 2014. 1, 2
- [16] G. Griffin, A. Holub, and P. Perona. Caltech-256 object category dataset. Technical report, California Institute of Technology, 2007. 7
- [17] A. Krizhevsky, I. Sutskever, and G. E. Hinton. ImageNet classification with deep convolutional neural networks. In *NIPS*, volume 25, 2012. 1, 2
- [18] D. J. C. MacKay. Bayesian interpolation. *Neural Computation*, 4(3):415–447, 1992. 2, 3
- [19] M.-E. Nilsback and A. Zisserman. Automated flower classification over a large number of classes. In *Proceedings of the Indian Conference on Computer Vision, Graphics and Image Processing*, 2008. 7
- [20] S. Nowak, K. Nagel, and J. Liebetrau. The CLEF 2011 photo annotation and concept-based retrieval tasks. In *CLEF Workshop Notebook Paper*, 2011. 7
- [21] M. Oquab, L. Bottou, I. Laptev, and J. Sivic. Learning and transferring mid-level image representations using convolutional neural networks. In *CVPR*, 2014. 1, 2, 6
- [22] A. Quattoni and A. Torralba. Recognizing indoor scenes. In *CVPR*, 2009. 7
- [23] A. S. Razavian, H. Azizpour, J. Sullivan, and S. Carlsson. CNN features off-the-shelf: An astounding baseline for recognition. In *CVPR Workshops*, 2014. 1, 2, 6
- [24] R. Rifkin, G. Yeo, and T. Poggio. Regularized least-squares classification. *Nato Science Series Sub Series III Computer and Systems Sciences*, 190:131–154, 2003. 2
- [25] P. Sermanet, D. Eigen, X. Zhang, M. Mathieu, R. Fergus, and Y. LeCun. OverFeat: Integrated recognition, localization and detection using convolutional networks. In *ICLR*, 2014. 1, 2
- [26] K. Simonyan and A. Zisserman. Very deep convolutional networks for large-scale image recognition. In *ICLR*, 2015. 2, 6
- [27] J. Snoek, H. Larochelle, and R. P. Adams. Practical Bayesian optimization of machine learning algorithms. In *Advances in Neural Information Processing Systems*, pages 2951–2959, 2012. 2
- [28] J. A. K. Suykens and J. Vandewalle. Least squares support vector machine classifiers. *Neural Processing Letters*, 9(3):293–300, 1999. 2
- [29] C. Szegedy, W. Liu, Y. Jia, P. Sermanet, D. A. S. Reed, D. Erhan, V. Vanhoucke, and A. Rabinovich. Going deeper with convolutions. *arXiv:1409.4842v1*, 2014. 2
- [30] T. Van Gestel, J. A. K. S. B. Baesems, S. Viaene, J. Vanthienen, G. Dedene, B. De Moor, and J. Vandewalle. Benchmarking least squares support vector machines classifiers. *Machine Learning*, 54(1):5–32, 2004. 2
- [31] T. Van Gestel, J. A. K. Suykens, G. Lanckrie, A. Lambrechts, B. D. Moor, and J. Vandewalle. Bayesian framework for least-squares support vector machine classifiers, gaussian processes, and kernel fisher discriminant analysis. *Neural Computation*, 14(5):1115–1147, 2002. 2, 3
- [32] C. Wah, S. Branson, P. Welinder, P. Perona, and S. Belongie. The Caltech-UCSD Birds-200-2011 dataset. Technical report, California Institute of Technology, 2011. 7
- [33] Z. Wu, Y. Zhang, F. Yu, and J. Xiao. A GPU implementation of GoogLeNet. Technical report, Princeton University, 2014. 6
- [34] J. Xiao, J. Hays, K. A. Ehinger, A. Oliva, and A. Torralba. SUN database: Large-scale scene recognition from abbey to zoo. In *CVPR*, 2010. 7
- [35] B. Yaho, X. Jiang, A. Khosla, A. L. Lin, L. J. Guibas, and L. Fei-Fei. Action recognition by learning bases of action attributes and parts. In *ICCV*, 2011. 7
- [36] M. D. Zeiler and R. Fergus. Visualizing and understanding convolutional networks. In *ECCV*, 2014. 2, 6
- [37] N. Zhang, M. Paluri, M. Ranzato, T. Darrell, and L. Bourdev. PANDA: Pose aligned networks for deep attribute modeling. In *CVPR*, 2014. 6
- [38] N. Zhang, J. Donahue, R. Girshick, and T. Darrell. Part-based R-CNNs for fine-grained category detection. In *ECCV*, 2014. 1, 2, 6
- [39] P. Zhang and J. Peng. SVM vs regularized least squares classification. In *ICPR*, 2004. 2
- [40] B. Zhou, A. Lapedriza, J. Xiao, A. Torralba, and A. Oliva. Learning deep features for scene recognition using places database. In *Advances in Neural Information Processing Systems*, pages 487–495, 2014. 2